SSIM 2023 – PM Dight (ed.)
© 2023 Australian Centre for Geomechanics, Perth, ISSN 3083-399X
doi:10.36487/ACG_repo/2335_20

Multistage triaxial testing of intact rock: volumetric strain-based methods applied to rock slope design

K Koosmen *PSM, Australia*

M Serati *The University of Queensland, Australia*

B Craig *Glencore, Australia*

Abstract

Triaxial testing of intact rock is commonly undertaken to provide input parameters for rock slope design. Multistage triaxial tests offer economies in terms of time, sample quantities and costs, and for these reasons have found commonplace in engineering practice. Volumetric strain-based methods are sometimes employed for multistage testing to minimise damage accumulation in early test stages. This is done by (1) terminating early test stages at volumetric strain reversal, (2) straining the final stage until failure occurs, then (3) inferring a peak stress for the earlier stages based on a correction factor derived from the final stage.

This paper provides a review of multistage triaxial testing along with fundamental rock mechanics theories that underpin the volumetric strain-based multistage testing method. Results from single and multistage tests are then used to demonstrate possible errors that may result if multistage tests are conducted over a range of stresses where compressive failure of intact rock is controlled by different failure mechanisms. Finally, some examples and discussion are provided to demonstrate the possible impact that these errors may have on rock slope stability assessments.

Keywords*: intact rock strength, triaxial testing, multistage methods, rock fracture mechanics*

1 Introduction

1.1 Context

Triaxial testing of intact rock is used to provide input parameters for the design of rock structures. For open pit slope design the intact rock strengths are primarily used as input parameters to estimate rock mass strengths using continuum-based methods such as the generalised Hoek–Brown criterion (Hoek & Brown 2018). Less commonly, the intact strength may also be used to estimate the strength of discrete blocks of intact rock in discontinuum-based models. Other parameters such as residual strengths, modulus and Poisson's ratio may also be of interest, depending on the application.

Single-stage triaxial tests provide a measure of the intact strength by applying a lateral confining stress (σ_3) to a core specimen before increasing the axial stress (σ_1) until failure occurs. The σ_1 value at failure is then taken as the peak intact strength (σ_p). This process destroys the core specimen and, consequently, each test only provides a single measurement of peak strength for the nominated confining stress.

Multistage techniques are fundamentally similar to single-stage techniques except the individual test stages are terminated before failure is induced. This preserves the specimens so that testing can be undertaken across a range of confining pressures. Benefits of this approach are:

- Multistage tests are cheaper, faster and require less samples to provide the same number of data points when compared to single-stage tests.
- A failure envelope can be defined from a single specimen when using multistage techniques.

- Conducting several multistage tests can provide several failure envelopes to better understand strength and parameter variability.

Multistage tests have historically employed 'imminent failure' methods based on the early work of Kovari & Tisa (1975). This involves monitoring the stress-strain curve throughout the test to infer the point when failure is imminent so the stage can be terminated to preserve the specimen for testing in later stages (see stress paths on the left of Figure 1). Use of imminent failure methods is often met with scepticism as selecting the point of imminent failure is subject to human error, and the growth of microcracks during earlier test stages may induce some damage in the specimen for later test stages. Both factors may lead to an underestimation of the peak strengths during later test stages.

An alternative method which seeks to overcome these issues is to terminate the early test stages at volumetric strain reversal (VSR) where the stress (σ_{VSR}), is significantly lower than the peak stress at failure. The VSR criterion allows for automation of stage termination while also limiting microcrack growth by not testing to 'imminent failure'. Failure is then induced during the final test stage where a stress ratio (Orilogi 2019; Venter et al. 2019) or stress magnitude (Pagoulatos 2004) is calculated, then applied to data from earlier tests stages to infer peak strengths at the lower confining stresses. Stres paths for this method are shown on the right of Figure 1, with equations to calculate peaks strengths shown in Equations 1 and 2.

Ratio corrected $$\sigma_{p.nf} = \sigma_{VSR.nf} \times \frac{1}{(\sigma_{VSR.f} \,/\, \sigma_{p.f})}$$ VSR stress ratio from final stage (1)

Magnitude corrected $$\sigma_{p.nf} = \sigma_{VSR.nf} \times (\sigma_{p.f} - \sigma_{VSR.f})$$ VSR stress magnitude from final stage (2)

where:

$\sigma_{p.nf}$ = calculated peak strength in non-final test stage.

$\sigma_{p.f}$ = measured peak strength in final test stage.

$\sigma_{VSR.nf}$ = stress at VSR measured in non-final test stage.

$\sigma_{VSR.f}$ = stress at VSR measured in final test stage.

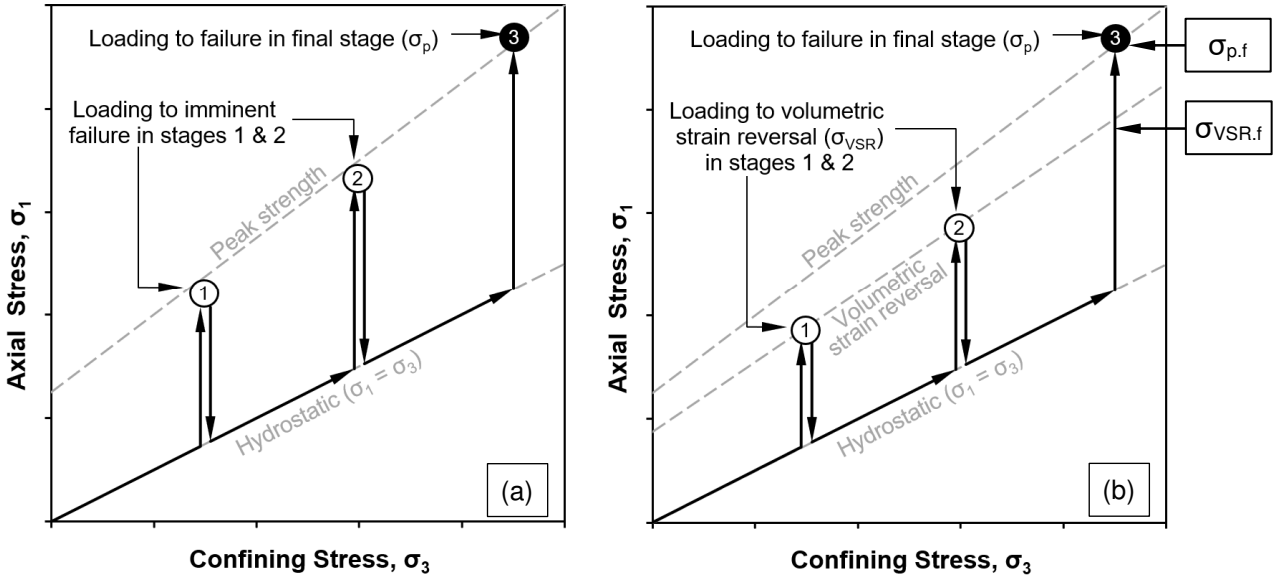

Figure 1 Stress paths for multistage triaxial test. (a) Imminent failure method; (b) Volumetric strain-based method

To date, the literature and experience with volumetric strain-based methods are limited compared to imminent failure methods. Furthermore, a fundamental assumption of the volumetric strain-based method is that the correction factors derived from the final test stage are applicable to all earlier test stages despite the changes in confining stress and the fracture mechanics which govern the brittle failure process.

1.2 Purpose

The purpose of this paper is to provide a review of volumetric strain-based methods for multistage triaxial testing to assess their suitability for use in rock slope stability assessments. This is done by comparing results from multistage triaxial tests with results from single-stage triaxial tests to understand what type of errors may be incurred due to the multistage test methodology. The experimental data is then used to draw conclusions on the validity of applying a single correction factor over a wide range of confining stresses to calculate peak strength in the non-final test stages. Lastly, two examples are provided to illustrate how errors associated with the peak intact strength may impact on slope stability assessments for open pit slope designs.

2 Rock mechanics theory

2.1 Hoek–Brown criterion

The Hoek–Brown failure criterion provides a non-linear relationship for peak strength of intact rock subject to brittle failure processes. The criterion was developed by Hoek & Brown (1980a; 1980b) using Griffith's criterion as a theoretical basis, then applying trial and error to empirically fit a parabolic envelope to a wide range of intact rock testing data (Hoek et al. 1995). The criterion is written in the principal stress space as shown in Equation 3:

Hoek–Brown criterion

$$\text{n } \sigma_1 = \sigma_3 + \sigma_{ci}\left[\frac{\sigma_3 m_i}{\sigma_{ci}} + s\right]^a \tag{3}$$

where:

- σ_1 & σ_3 = major and minor principal stresses.
- σ_{ci} = is the unconfined compressive strength.
- m_i = fitting parameter, usually varying between 5 and 40 depending on rock type.
- s and a = fitting parameters, usually taken as 1 and 0.5, respectively, for intact rock.

Curve fitting of triaxial data can be undertaken by manually modifying σ_{ci} and m_i until a suitable fit is obtained with the experimental data, or more rigorous regression analyses can be used such as those listed by Mostyn & Douglas (2000). Figure 2 illustrates how the Y-intercept of the Hoek–Brown envelope is controlled by σ_{ci} while the gradient is controlled by m_i. In this respect, σ_{ci} and m_i are analogous to the cohesion and friction angle of the linear Mohr–Coulomb criterion (Hoek 1983). It should also be noted that the Hoek–Brown criterion is only applicable to brittle, and not ductile, failure of intact rock. The transition from brittle to ductile failure can be approximated by Mogi's line (Mogi 1966; $\sigma_1 = 3.4\sigma_3$).

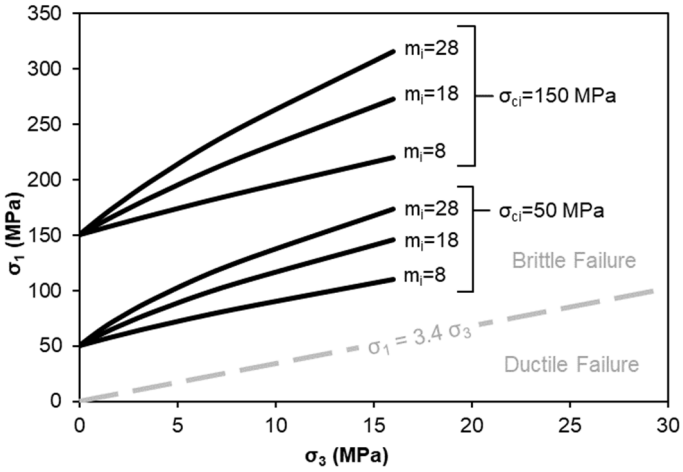

Figure 2 Effect of input parameters on the slope and intercept of the Hoek–Brown criterion

2.2 Microcracking of intact rock during compression

Modern concepts of brittle rock fracture are founded in the works of Griffith (1920, 1924) who studied the fracture mechanics of glass windshields. Griffith proposed that (1) brittle solids contain randomly orientated microcracks (named Griffith cracks), and (2) that tensile fractures (named wing cracks) nucleate from the tip of Griffith cracks in a direction that is parallel to the major principal stress axis. For the case of intact rock, the wing cracks may nucleate from pre-existing microcracks in the rock, or along other flaws such as grain boundaries, cleavage within minerals, stiff or soft inclusions, and low-aspect ratio cavities (Horii & Nemat-Nasser 1985; Tang & Hudson 2011; Kaiser & Kim 2014). Griffith's original theoretical criteria are now recognised to be of limited practical value in rock engineering (Hoek & Martin 2014), however, the mechanism of tensile wing cracks propagating from a flaw in the microstructure remains a fundamental concept in the brittle rock failure.

Under low confining stress the wing cracks propagate extensively in a direction parallel to the major principal stress. This leads to axial splitting failures, for example, as commonly observed in the laboratory during uniaxial compressive strength (UCS) testing, or in the field as rockburst or spalling at the boundaries of underground excavations. Under higher confining stresses the wing cracks may still develop but their growth is supressed in the axial direction due to the effects of confinement (Einstein & Dershowitz 1990; Gupta & Bergstrom 1998; Horii & Nemat-Nasser 1985; Kaiser & Kim 2014). This supresses the growth of individual wing cracks but facilitates the growth of wing cracks from neighbouring flaws which form clusters and preferentially align in an en echelon arrangement to form a shear zone, leading to ultimate shear failure (Gupta & Bergstrom 1998). Shear failure is therefore the dominant mode of failure during triaxial compression at higher confining stresses. The reader is referred to Hoek & Martin (2014) for further discussion of these concepts.

2.3 Crack thresholds for intact rock

The brittle fracture of intact rock occurs from the development, growth and coalescence of microcracks. Based on the works of numerous authors (Hoek 1965; Brace et al. 1966; Bieniawski 1967; Lajtai 1974; Tapponier & Brace 1976; Gramberg 1989; Lockner et al. 1992; Martin 1993; Martin & Chandler 1994; Martin 1997; Eberhardt et al. 1998), the microcrack development is characterised by three distinct stress thresholds which divide the stress-strain curve into four distinct zones. The stress thresholds are (see Figure 3):

- Crack closure (σ_{cc}) – the stress when most of the pre-existing microcracks are closed. The stress-strain curve is non-linear leading up to crack closure and linear-elastic immediately following.
- Crack initiation (σ_{ci}) – the stress where small and randomly distributed microcracks begin to develop throughout the rock, corresponding to the end of linear-elastic behaviour.
- Crack damage (σ_{cd}) – defining the onset of uncontrolled crack growth when individual cracks lengthen and/or coalesce with other cracks. Macro-scale failure then occurs by axial splitting or shear when the critical crack density is exceeded.

The σ_{ci} threshold depends on rock type and which method is used to determine or infer σ_{ci}, however, typical values are 30 to 60% of the peak strength during unconfined compression, and 40 to 80% of the peak strength during confined compression (Nicksiar & Martin 2013; Mutaz et al. 2021).

The σ_{cd} threshold also varies for different rock types and the determination method, and corresponds with the point of VSR on the stress-strain curve as seen Figure 3 (Brace et al. 1966; Bieniawski 1967; Martin 1993). Typical values of σ_{cd} are between 65 to 90% of the peak strength during unconfined compression and 60 to 100% of the peak strength in confined compression (Diederichs et al. 2009; Taheri et al. 2020).

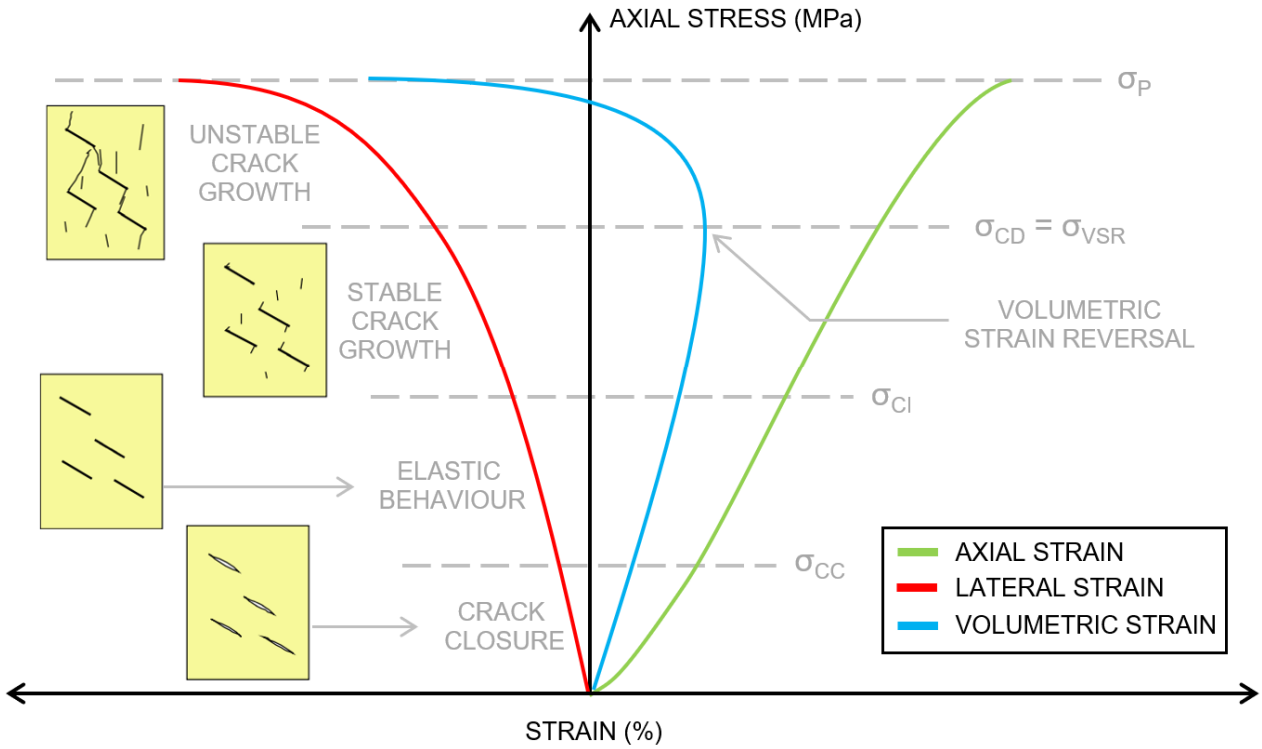

Figure 3 Idealised stress-strain curve illustrating the stages of microcracking and stress thresholds

3 Laboratory testing

3.1 Methodology

Single and multistage triaxial tests were conducted under varying conditions so that the single-stage tests could be used as a control group for validation of the multistage tests. All tests were conducted on sandstone specimens that were collected from a coal deposit in Northern Queensland, Australia. All samples were collected from the same unit within the stratigraphy and with the same lithology (sandstone), with a field-estimated strength of R2 to R3 and with a density in the range of 2.54 to 2.61 t/m^3. The triaxial testing was conducted using a stiff-framed GCTS RTR2500 triaxial machine fitted with a closed-loop servo-controlled loading system. This allowed for automation of the testing procedure according to instantaneous stress-strain measurements. Linear variable differential transformers were used to measure the circumferential and axial strains during each test.

A summary of the testing schedule is provided in Table 1, with additional details as follows:

- The dataset for the single-stage triaxial tests (Group 2) included data points from 33 single-stage tests plus nine data points from the final stage of the multistage tests. These multistage results were included in the single-stage dataset assuming minimal ‘damage’ accumulation in early stages of the multistage tests. Therefore, the final stages are effectively the same as a single-stage test.
- The multistage test results were conducted across two stress ranges, where the Group 3 tests were conducted at lower confining stresses of 2 to 6 MPa, and the Group 4 tests were conducted at higher confining stresses of 6 to 24 MPa.
- All multistage test stages were terminated at VSR in the non-final stages, then tested to failure in the final test stage (i.e. per the stress paths in Figure 1a).
- The peak strength for non-final stages of the multistage tests were then calculated using both the ratio and magnitude correction factors as shown by Equations 1 and 2.

Table 1 Schedule of triaxial testing

Group	Test type	Confining stress (MPa)	# of data points
1	Uniaxial compressive strength	0	29
2	Single-stage triaxial	0.5, 2, 6, 10, 15, 24	33 + 9 [2] = 42
3	Multistage triaxial [1]	2, 4, 6 (low stress range)	15 (= 5 tests × 3 stages)
4	Multistage triaxial [2]	6, 12, 18, 24 (higher stress range)	16 (= 4 tests × 4 stages)

[1] Using volumetric strain reversal as stage termination criteria in the non-final stages
[2] The single-stage dataset includes nine results from the final stage of each multistage test. See further discussion in text.

3.2 Single-stage test results

Results from the single-stage triaxial tests (Group 2) are plotted in Figure 4 where a Hoek–Brown envelope is fitted to the average stress points, giving σ_{ci} of 39 MPa and m_i of 9. The σ_{ci} value of 39 MPa from curve fitting compares very well with the median UCS value of 38 MPa. The VSR stress ratios and VSR stress magnitudes are included in Figure 5 and discussed in more detail in the following sections.

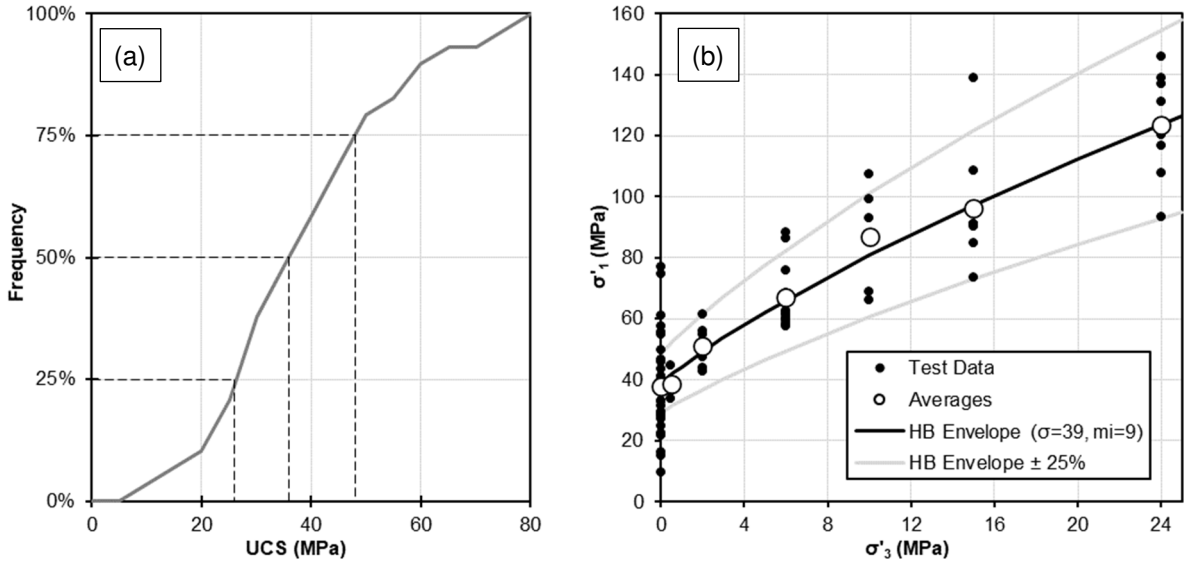

Figure 4 (a) Cumulative distribution from uniaxial compressive strength (UCS) testing; (b) peak strength envelope based on UCS and single-stage triaxial testing

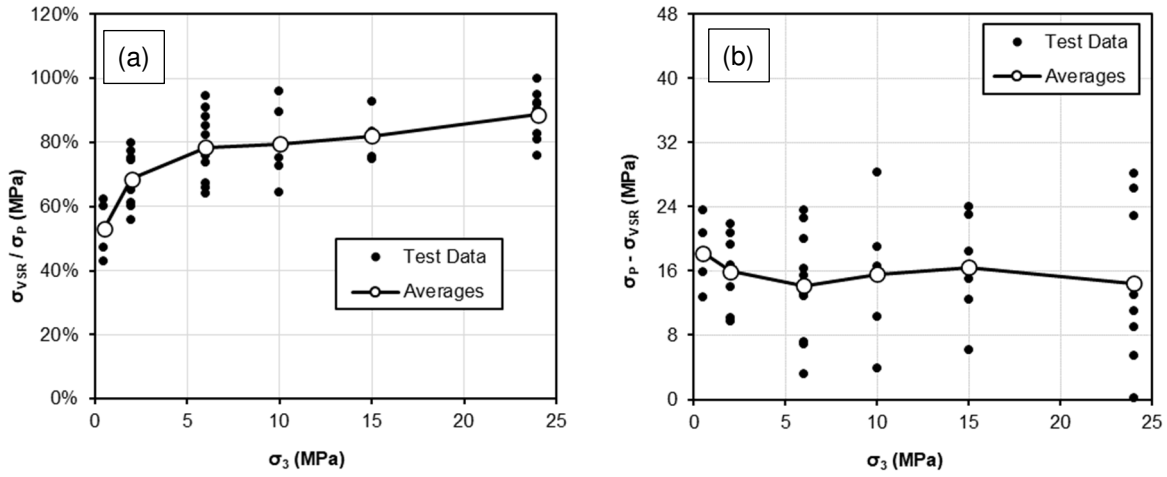

Figure 5 Results from single-stage triaxial testing showing (a) Volumetric strain reversal (VSR) stress ratio; (b) VSR stress magnitude

3.3 Multistage test results

Hoek–Brown failure envelopes were determined from the multistage tests and are shown in Figure 6 for the ratio corrected peak strengths, and in Figure 7 for magnitude corrected peak strengths. The Hoek–Brown intact strength parameters (σ_{ci} and m_i) for all failure envelopes are summarised in Table 2.

Across both datasets the average strength that was measured in the test final stage (6 and 24 MPa) is comparable with the strength envelope defined from the single-stage tests. This indicates that the multistage specimens have a similar average strength to the single-stage specimens, and that any significant deviations between the multistage and single-stage failure envelopes are therefore not caused by strength variability.

When the ratio correction factor is used for the low stress tests (Figure 6a) it is seen that there is an increase in the apparent error as the confining stresses reduce. Similar trends are also observed for the higher stress tests (Figure 6b), although the apparent error is less pronounced than what is seen for low stress tests in Figure 6a.

In both datasets the apparent error is attributed to variability of the VSR stress ratio across different confining stresses, which is evident from the single-stage test data that is shown in Figure 5a. If a higher ratio is derived in the final stage, then applied at lower confining stress where a lower ratio is appliable, the net effect will be that the calculated peak strengths underestimate the true peak strength at lower confining stresses. As an example, consider the data from the single-stage tests where average ratios of 65% and 80% are measured at 2 and 6 MPa. If peak strengths at 2 MPa are calculated using Equation 1 and the 80% ratio then the peak strength will be 1.25 x σ_{VSR}. If the 'correct' ratio of 65% is considered for 2 MPa then the peak strength will be equal to 1.54 x σ_{VSR}. The apparent errors in the multistage results from Figure 6 are therefore caused by assuming that the ratio correction factors derived from the final test stages are constant across all stages where, in fact, the ratio is variable across a range of confining pressures. At this stage it is hypothesised that the change in ratio with confining pressure may be related to a change in failure mechanism from tensile to shear-dominated failure processes for intact rock, although further work is required to confirm this theory.

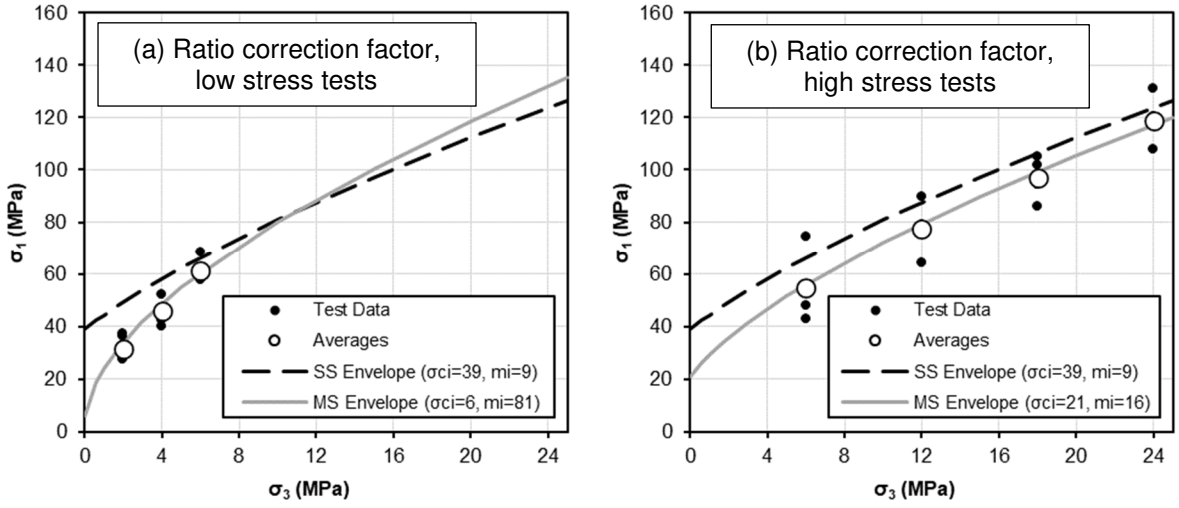

Figure 6 Multistage test results where the ratio correction factor was used to calculate peak strengths. (a) Lower stress tests with σ_3 = 2–6 MPa; (b) Higher stress tests with σ_3 = 6–24 MPa

The magnitude corrected multistage results are shown in Figure 7 and give a better comparison with the single-stage results than what was seen for the ratio corrected results in Figure 6. Tests conducted at lower confining pressures (Figure 7a) still show considerable variability from the single-stage envelope, while tests at higher confining pressures (Figure 7b) align very closely with the single-stage envelope. These outcomes are explained using the results from the single-stage triaxial tests in Figure 5b, where the average stress magnitude values for this rock type show minimal variability across a wide range of confining pressures and with the greatest variation in the low stress range.

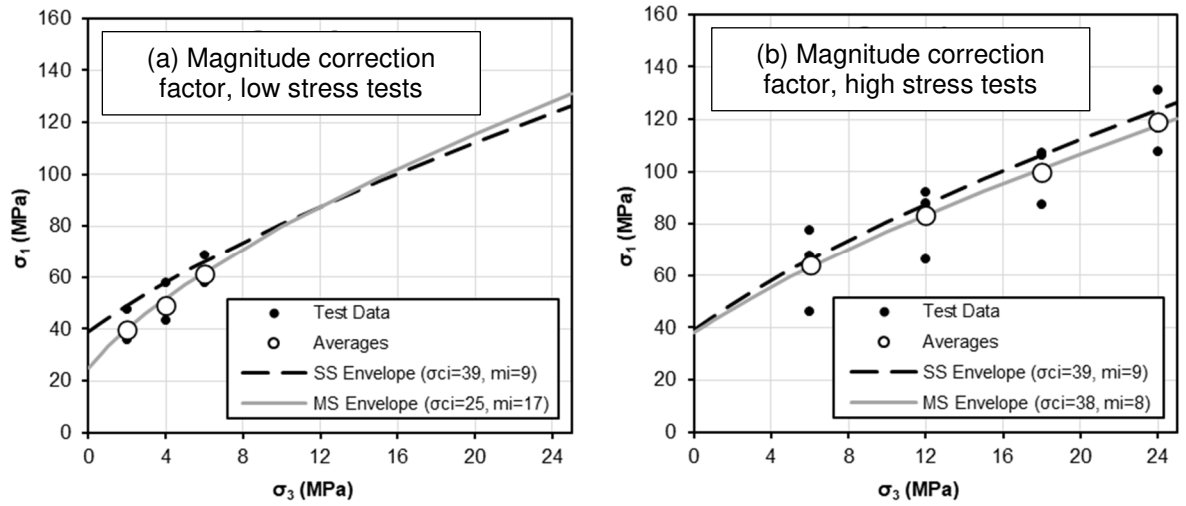

Figure 7 Multistage results where the magnitude correction factor was used to calculate peak strengths. (a) Lower stress tests with σ_3 = 2–6 MPa; (b) Higher stress tests with σ_3 = 6–24 MPa

Table 2 Hoek–Brown parameters determined from single-stage and multistage triaxial testing

Test type	Confining stress	Peaks strengths calculated from	σci (MPa)	mi	See figure
Single-stage	σ_3 = 0–24 MPa	–	39	9	4b
Multistage	σ_3 = 2–6 MPa	VSR stress ratio	6	81	6a
Multistage	σ_3 = 6–24 MPa	VSR stress ratio	21	16	6b
Multistage	σ_3 = 2–6 MPa	VSR stress magnitude	25	17	7a
Multistage	σ_3 = 6–24 MPa	VSR stress magnitude	38	8	7b

3.4 Main findings from laboratory testing

The main findings from the laboratory testing are:

1. The VSR stress ratio (σ_{VSR}/σ_P) and VSR stress magnitude ($\sigma_P - \sigma_{VSR}$) can vary with confining pressure. The maximum variability appears to occur in the low stress range and may be related to a transition between tensile and shear-dominated fracture processes.
2. Use of a ratio or magnitude correction factor calculated from the final stage of a multistage test may introduce errors if used to calculate peak strengths in the non-final stages of a multistage test.
3. For the sandstone material considered in the experiments above, it was found that:
    a. The magnitude correction was more accurate than the ratio correction factor for calculating peak strengths from multistage tests when compared to the measured peak strengths from single-stage testing.
    b. Peak strengths calculated from the multistage tests using the ratio and magnitude correction factors incurred less error when tests were conducted at higher confining stresses.

4 Other rock types

The laboratory testing and results discussed in Section 3 have only considered a single rock type. Additional data was therefore sourced from the literature, then analysed to provide a better understanding on how the ratio and magnitude correction factors perform for predicting peak strengths across different rock types. The process was as follows:

1. Single-stage triaxial test data was sourced for various rock types where σ_{VSR} and peak strength were reported across a wide range of confining pressures. Average data points were calculated where datasets contain several data points at a single confining pressure.
2. A ratio correction factor and magnitude correction factor were determined from the test or data point that corresponds to the maximum confining pressure.
3. The ratio and magnitude correction factors were then applied to σ_{VSR} recorded for all other stage tests to calculate peak strengths at lower confining pressures.
4. Hoek–Brown envelopes were then fitted to the calculated peak strengths and measured peak strengths to enable a comparison of the datasets.

The peak strength envelopes and intact parameters (σ_{ci} and m_i) are shown in Figure 8 for non-sedimentary rocks and Figure 9 for sedimentary rocks. A summary of how the calculated peak strength envelopes compare with the measured peak strength envelopes is provided in Table 3. A good fit is obtained where the calculated peak strength envelope compares well with the measured peak strength envelope, and where the maximum error is less than a nominal value of around 15%. Where these criteria are satisfied it is implied that the ratio or magnitude correction factor is reasonably constant across the applied stress range.

Table 3 Comparison of calculated peak strength envelopes with measured peak strength envelopes

		Maximum error [1]		Goodness of fit between failure envelopes [2]			
See Figure	**Rock type**	**Error for ratio corrected failure envelope**	**Error for magnitude corrected failure envelope**	**Reasonable fit for ratio and magnitude corrected envelopes**	**Reasonable fit only for ratio corrected failure envelope**	**Reasonable fit only for magnitude corrected failure envelope**	**Poor fit for ratio and magnitude corrected envelopes**
8a	B. Granite	-24%	39%				✓
8b	LdB Granite	15%	74%		✓		
8c	Marble	-9%	33%		✓		
8d	Basalt	-13%	-2%	✓			
9a	Sandstone	-46%	-5%			✓	
9b	Sandstone	-55%	51%				✓
9c	B4 Shale	28%	41%				✓
9d	Shale	8%	27%		✓		

[1] Max error is obtained in all cases where σ_3=0 MPa, and is the percentage difference between the σ_{ci} value from the calculated and measured peak strength envelopes. Negative/positive errors indicate an under/overestimate of the measured peak strength.
[2] Refers to a comparison between the measured peak strength envelope from the single-stage tests and the calculated peak strength envelope/s from the multistage tests.

The observed trends for the different rock types are as follows:

- Variable results are observed where calculated failure envelopes compare well with the measured failure envelopes for some rock types, but not for others.
- The ratio corrected peak strength envelopes provide a reasonable fit to the measured peak strength envelope in four out of the eight cases (Beishan granite, marble, basalt and shale). Otherwise there is generally an underestimate of peak strength (LdB granite, and two sandstones). There is only one instance where the ratio corrected envelope significantly overestimates the measured peak strength envelope (b4 shale).

- The magnitude corrected peak strengths tended to overestimate the measured peak strengths in most cases, with a maximum error of up to 74% for Beishan granite (Figure 8b). There were only two of eight instances where the magnitude corrected envelope provided a reasonable fit to the measured peak strength envelope (basalt, Figure 8d; and Berea sandstone, Figure 9a).
- It is concluded that neither of the methods are universally reliable for calculating peak strengths across the range of rock types that are considered.
- Where large errors are observed, this outcome is attributed to the ratio correction factor or magnitude correction factor not being constant over the applied range of confining pressures.

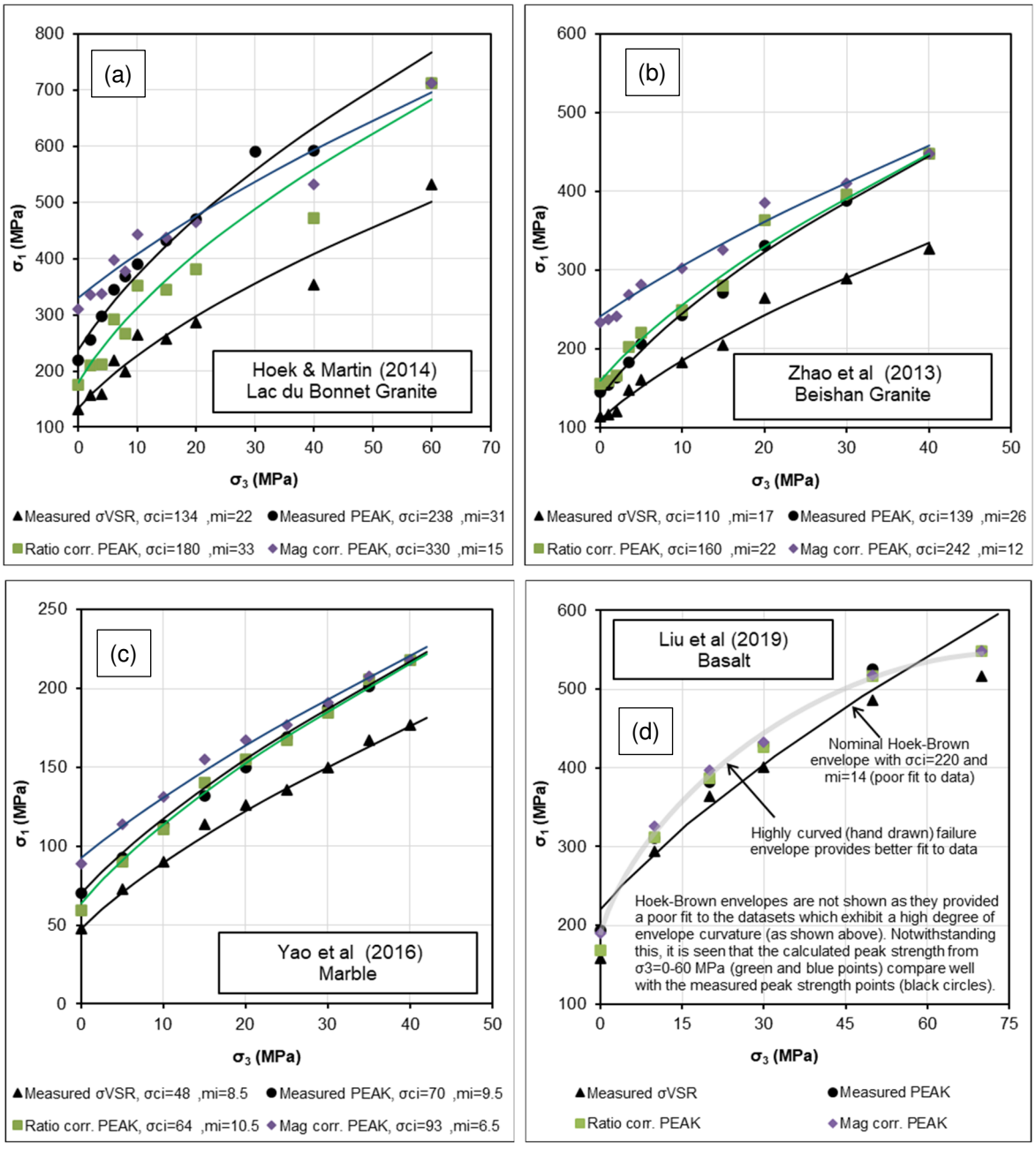

Figure 8 Results from single-stage triaxial tests sourced from the literature for non-sedimentary rocks where peak strengths have been calculated using the ratio and magnitude correction factors, then compared with measured peak strengths

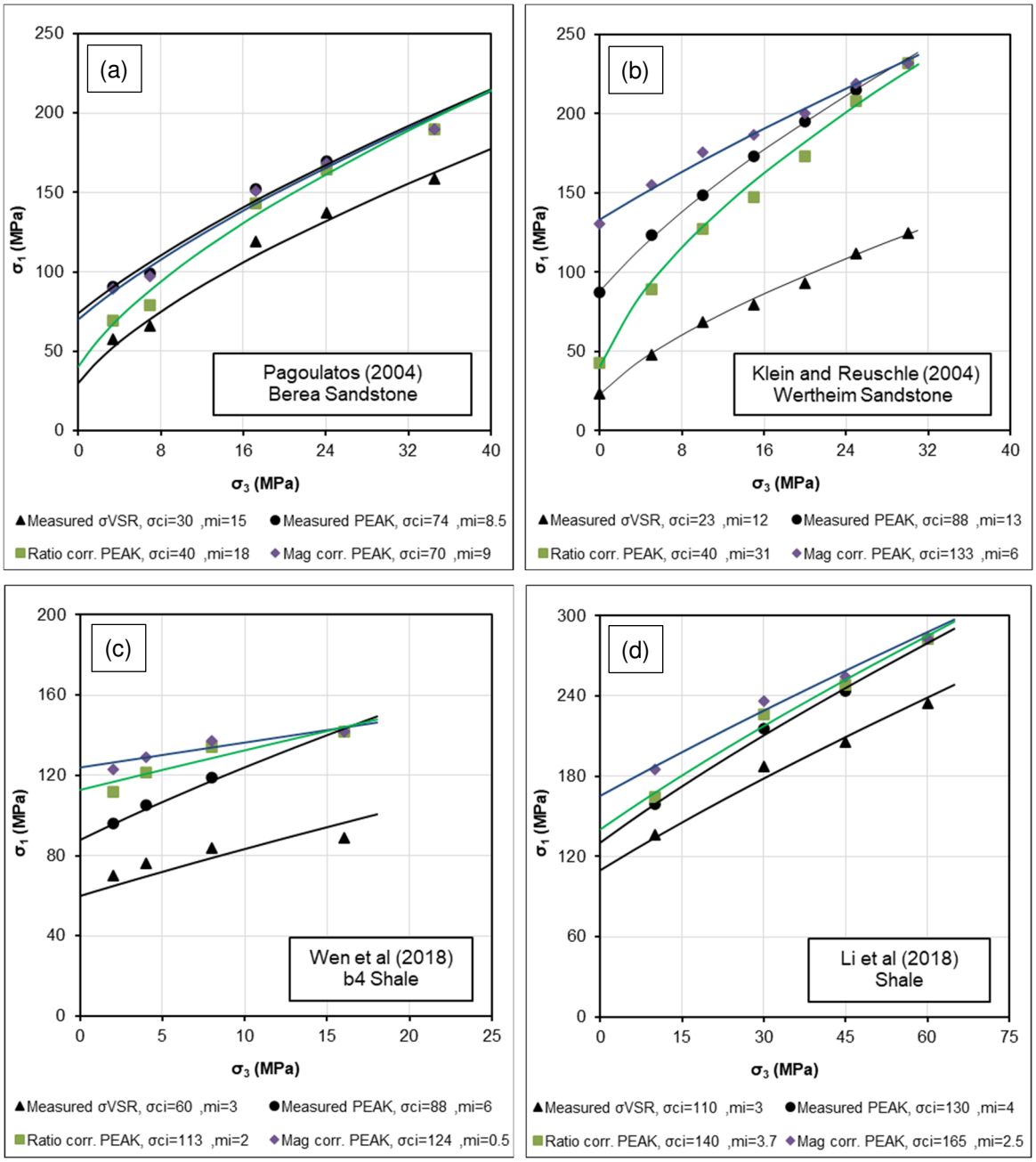

Figure 9 Results from single-stage triaxial tests sourced from the literature for sedimentary rocks where peak strengths have been calculated using the ratio and magnitude correction factors, then compared with measured peak strengths

5 Implications for rock slope stability assessments

Data from Sections 3 and 4 have demonstrated that errors of varying degree can be incurred when using volumetric strain-based methods to calculate peak intact rock strengths from multistage triaxial tests. The magnitude of the error depends on (1) the rock type, (2) the range of confining stress over which the tests are conducted and (3) whether the ratio correction or magnitude correction factors are applied to calculate the peak strengths. But what do these errors mean with respect to rock slope stability estimates? Are the impacts significant or trivial?

Generally speaking, the most significant impacts can be expected for failure mechanisms where rock mass strengths significantly contribute to the stresses that resist slope failure. Two simplified cases are used to illustrate this where 2D limit equilibrium techniques have been used to estimate to the Factor of Safety (FOS).

Case 1 considers a highwall slope where the failure mechanism is an active-passive wedge with basal sliding along a weak horizontal plane and with the back scarp extending through the rock mass. Case 2 considers a footwall slope with sliding along a weak inclined plane with breakout through the rock mass in the toe region. Model geometries are shown in Figure 10, with additional assumptions as follows:

- Mohr–Coulomb strength parameters for the weak structure were c' = 0 kPa and ϕ' = 15°.
- Pore pressures were estimated using a steady state flownet.
- Rock mass strengths were based on the generalised Hoek–Brown criterion (Hoek & Brown 2018).
- The geological strength index (GSI) for the rock mass was 65.
- The blast disturbance factor (D) was zero.
- Different combinations of intact strength parameters (σ_{ci} and m_i) are adopted based on the combinations derived from the single-stage and multistage triaxial testing described in Section 3.

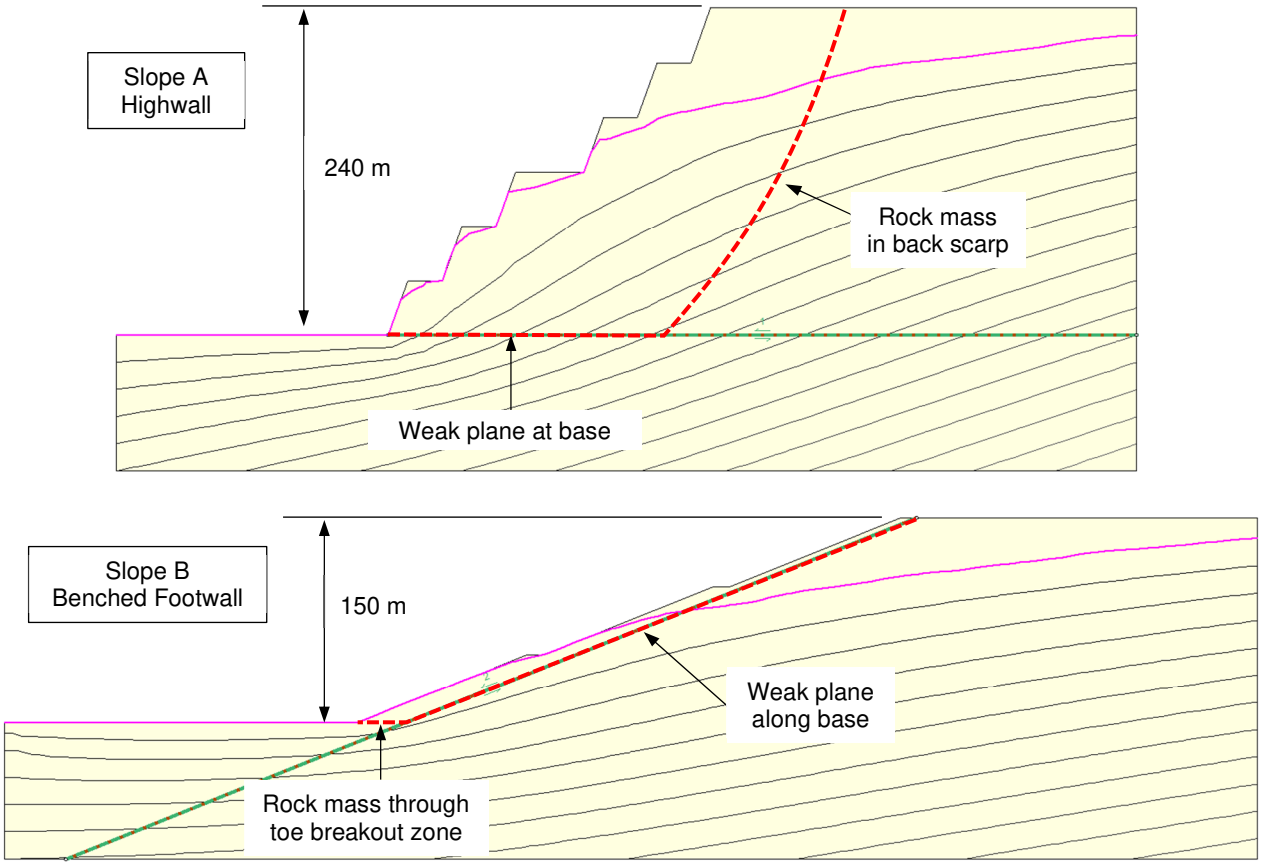

Figure 10 Highwall and footwall slopes with failure mechanisms considered for stability analysis. Contours show pore pressures estimated from flownet via finite element analysis

The intact strength parameters used for rock mass strength estimates are summarised in Table 4 along with the FOS values that were calculated for each case. For both slopes types the FOS is calculated to be around 1.5 where the single-stage triaxial test results are used as the basis for rock mass strength estimates (scenario 1). The single-stage tests are considered to provide the most reliable estimate of intact strength. Therefore, the scenario 1 results are used as the basis to calculate the error for the other scenarios.

Table 4 Intact rock strengths used to define rock mass strengths with calculated FOS values for the two different slope configurations

Scenario	Triaxial test data from Section 3 used to define rock mass strengths					Slope A – highwall FOS [1]	Slope B – footwall FOS [1]
	Test type	Correction method used to calculate peak strength	σ_3 range (MPa)	σ_{ci} (MPa)	mi		
1	SS TXL	N/A (measured directly)	0.5 – 24	39	9	1.48	1.54
2	MS TXL	Stress ratio	0 – 6	6	81	1.22 (18%)	1.09 (29%)
3	MS TXL	Stress ratio	6 – 24	21	16	1.32 (11%)	1.23 (20%)
4	MS TXL	Stress magnitude	0 – 6	25	17	1.38 (7%)	1.30 (16%)
5	MS TXL	Stress magnitude	6 – 24	38	8	1.46 (1%)	1.53 (1%)

[1] Value in brackets shows relative 'error' compared to the FOS that is calculated for scenario 1.

When the rock mass strengths are estimated using the intact strength parameters from the multistage tests (scenarios 2 to 5), it is seen that the FOS values are between 1% and 29% lower than what was calculated for scenario 1 based on the single-stage tests. Not surprisingly, the largest errors for both slopes were observed for scenario 2, where the multistage test results provided the largest underestimate of the peak intact strengths (Figure 6a). Furthermore, it was also seen that the footwall slope recorded larger errors than the highwall slope. This is because the strength errors associated with multistage tests tend to compound at lower confining stresses, and the average stress is lower in the rock mass component in the footwall slope than in the highwall slope. The error of 1% that is obtained for both slopes for scenario 5 is also to be expected, given that σ_{ci} and m_i are nearly identical to values that are used for scenario 1. However, and as illustrated in previous sections, it may not always be the case (and more likely is seldom the case) that there is such a close match between the single-stage and multistage test results. It is only with the benefit of single-stage testing that the results from scenario 5 are able to be validated, and without the single-stage tests it could not be confidently predicted whether scenario 2, 3, 4 or 5 is the valid case.

A final point to note is regarding the effects of GSI on rock mass strength estimates. The assessments above have utilised a GSI of 65 which corresponds to a reasonably good rock mass. When utilising the generalised Hoek–Brown criterion to estimate rock mass strengths it is found that rock mass strengths become less sensitive to the intact strength parameters as the GSI decreases. This is shown by Figure 11 where the intact strength parameters from scenarios 1 to 5 are used to calculate rock mass strengths for GSI values between 40 and 70. Maximum variability between the rock mass strength envelopes is observed when the GSI is 70 and the failure envelopes converge as the GSI reduces, despite the variable intact strength parameters.

The implications of this were tested using the footwall scenario from Table 4 (case B) and reducing the GSI from 65 to 42 for the rock mass strength estimates. For scenario 1 where the intact strength parameters are calculated from the single-stage triaxial tests, the FOS value was calculated to be 0.98. For scenarios 2 to 5, the FOS values ranged from 0.92 to 0.98 with a maximum error of 6% (relative to the FOS for scenario 1). This is a significant reduction in the maximum error of 29% that was recorded with an assumed GSI of 65, even though the same intact strength parameters are used.

The analyses presented above have demonstrated that:

- Errors with intact strength estimates resulting from multistage test methods may have significant impacts on the reliability of slope stability assessments.
- The impact of these errors is more pronounced for higher quality rock mass with higher GSI values if the generalised Hoek–Brown criterion is used to estimate rock mass strengths.

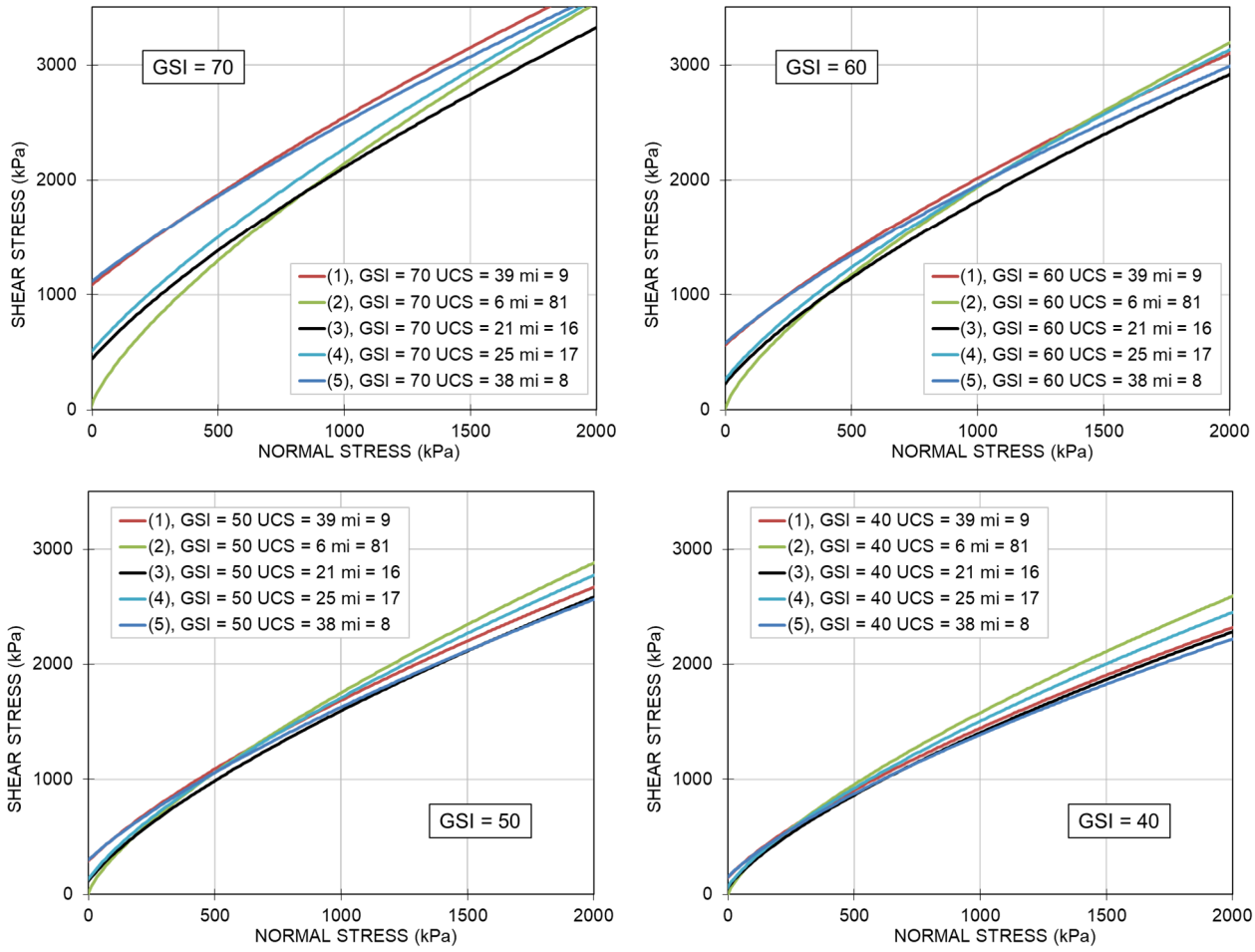

Figure 11 Rock mass failure envelopes calculated using the generalised Hoek–Brown criterion, with the same five sets of intact strength parameters (σ_{ci} and m_i) and considering different GSI values

6 Conclusion

The conclusions from this study are as follows:

- Single-stage triaxial tests provide the most reliable method for determining intact rock strength. While multistage techniques may be preferred in some instances due to constraints imposed by testing budgets and sample quantities, their use will incur a reduction in the reliability of the results.
- Volumetric strain-based techniques for multistage testing provide an alternative to the more conventional imminent failure techniques. These tests terminate the non-final test stages at VSR then calculate the peak strengths in these stages based on a VSR stress ratio or VSR stress magnitude correction factor which is determined from the final test stage.
- A fundamental assumption when applying these correction factors to calculate peak strength in the non-final test stages is that the correction factor is constant across the applied range of confining stresses.
- Results from this study have demonstrated that the correction factors may not be constant across a wide range of confining stresses for different rock types. The maximum rate of variability appears to occur in the low stress range and may be related to a transition between tensile and shear-dominated fracture processes.
- The experimental data reviewed in this study indicates that use of the VSR stress ratio or VSR stress magnitude as a correction factor can provide a reliable estimate of peak strength for some rocks,

but not for others. Moreover, it was demonstrated for some rock types that neither of the methods provide a reliable strength estimate. The maximum errors that are observed between the calculated and peak strengths tend to compound for lower confining stresses.

- There is no clear trend from the current results to provide an indication in advance on which correction factor may give a reliable results for a particular rock type. For example, it is not the case that use of the VSR stress ratio will always give reliable results for sandstone, igneous rocks or some other rock type, and likewise with VSR stress magnitude. The only way to confirm the reliability of the multistage methods is by undertaking parallel single-stage tests to enable a direct comparison of peak strengths from the single and multistage datasets.
- Intact rock strengths are commonly used to estimate rock mass strengths for assessing slope stability where key failure mechanisms include some element of failure through the rock mass. In these cases, significant errors with the calculated intact strengths from multistage tests may then introduce significant errors in slope stability estimates. All else being equal, the impact of intact strength errors on slope stability estimates will be more pronounced for higher quality rock masses with higher GSI values if the generalised Hoek–Brown criterion is used to estimate rock mass strengths. This is because rock mass strength estimates based on the Hoek–Brown criterion are more sensitive to variation of intact rock strength for higher GSI values.
- If volumetric strain-based techniques are to be used for multistage testing then it is recommended that (1) a series of UCS tests be included in the dataset to help constrain σ_{ci} on the Y-intercept, (2) that variable confining stresses are utilised for the final stage of different tests, and (3) that larger weightings are given to the final test stages where peak strength is directly measured and not calculated using a correction factor.
- This paper has demonstrated that large errors of more than 50% may occur when estimating peak intact rock strengths using volumetric strain-based techniques for multistage triaxial testing (see Table 3). Volumetric strain-based techniques are usually employed to minimise the perceived errors associated with the more conventional imminent-failure-based techniques. Given potential errors of more than 50%, the question must be asked: Are the volumetric strain-based techniques more or less reliable than the conventional imminent failure techniques? Further work is required to provide a broad assessment on the reliability of imminent failure techniques, however, it is the authors' opinion that maximum potential errors would probably be less than 50% with reasonable testing procedures. Undertaking a large suite of single-stage testing would help to eliminate the potential for errors associated with either of the multistage techniques.

References

Brace WF, Paulding, BW & Scholz, C 1966, 'Dilatancy in the fracture of crystalline rocks', *Journal of Geophysical Research*, vol. 71, no. 16, pp. 3939–3953.

Bieniawski, ZT 1978 'Determining rock mass deformability: experience from case histories', *International Journal of Rock Mechanics and Mining Sciences and Geomechanics Abstracts*, vol. 15, no.5, pp 237–247.

Diederichs, MS, Carter, T & Martin, D 2009, 'Practical rock spall prediction in tunnels', in *Proceedings of the International Tunnelling Association World Tunnel Congress*, pp. 1–8.

Eberhardt, E, Stead, D, Stimpson, B & Read, RS 1998, 'Identifying crack initiation and propagation thresholds in brittle rock', *Canadian Geotechnical Journal*, vol. 35, no. 2, pp. 222–233.

Einstein, EW & Dershowitz, WS 1990, 'Tensile and shear fracturing in predominantly compressive stress fields – a review', *Engineering Geology*, vol. 29, pp 149–172.

Gramberg, J 1989, *A Non-Conventional Review on Rock Mechanics and Fracture Mechanics*, CRC Press, Boca Raton.

Griffith, AA 1920, 'The phenomena of rupture and flow in solids', *The Philosophical Transactions of the Royal Society of London,* vol. 221, pp. 163–198.

Griffith, AA 1924, 'The theory of rupture', in CB Biezeno & JM Burgers (eds), P*roceedings of the First International Congress for Applied Mechanics*, Delft Tech, pp 55–63.

Gupta, V & Bergstrom, JS 1998, 'Compressive failure of rocks by shear faulting', Journal of Geophysical Research: Solid Earth, vol. 110, no. B10, pp. 23875–23895 .

Hoek, E 1965, *Rock Fracture Under Static Stress Conditions*, report for Council for Scientific and Industrial Research, MEG 383, Pretoria.

Hoek, E & Brown, ET 1980a, 'Empirical strength criterion for rock masses', Journal of the Geotechnical Engineering Division, ASCE, vol. 106, no. 9, pp 1013–1035.

Hoek, E & Brown, ET 1980b, *Underground Excavations in Rock*, Institute of Mining and Metallurgy, London.

Hoek, E 1983, 'The strength of jointed rock masses', *Geotechnique*, vol. 33, no. 3, pp. 187–222.

Hoek, E, Kaiser, PK & Bawden, WF 1995, *Support of Underground Excavation in Hard Rock*, A.A. Balkema, Rotterdam.

Hoek, E & Brown, ET 2018, 'The Hoek-Brown failure criterion and GSI – 2018 edition', *Journal of Rock Mechanics and Geotechnical Engineering*, vol. 11, is. 3, pp.445–463.

Hoek, E & Martin, CD 2014, 'Fracture initiation and propagation in intact rock – a review', *Journal of Rock Mechanics and Geotechnical Engineering*, vol. 6, no. 4, pp. 278–300.

Horii, H & Nemat-Nasser, S 1985, 'Compression-induced microcrack growth in brittle solids - axial splitting and shear failure', *Journal of Geophysical Research*, vol. 90, no. B4, pp. 3105–3125.

Kaiser, PK & Kim, BH 2014, 'Characterization of strength of intact brittle rock considering confinement-dependent failure processes', *Rock Mechanics and Rock Engineering*, vol. 48, pp. 107–119.

Kovari, K & Tisa, A 1975, 'Multiple failure state and strain controlled triaxial tests', *Rock Mechanics*, vol. 7, pp. 17–33.

Lajtai, EZ 1974, 'Brittle fracture in compression', *International Journal of Fracture*, vol. 10, pp. 525–536.

Lockner, DA, Moore, DE & Reches, Z 1992, 'Microcrack interaction leading to shear failure', paper presented at the 33rd U.S. Symposium on Rock Mechanics, Santa Fe, New Mexico.

Martin, CD 1993, *Strength of Massive Lac du Bonnet Granite Around Underground Openings*, PhD thesis, University of Manitoba, Winnipeg.

Martin, CD & Chandler, NA 1994, 'The progressive fracture of Lac du Bonnet granite', *International Journal of Rock Mechanics and Mining Sciences and Geomechanics Abstracts*, vol. 31, no. 6, pp. 643–659.

Martin, CD 1997, 'The effect of cohesion loss and stress path on brittle rock strength', *Canadian Geotechnical Journal*, vol. 34, no. 5, pp.698–725.

Mogi, K 1966, 'Pressure dependence of rock strength and transition from brittle fracture to ductile flow', *Bulletin Earthquake Research Institute*, vol. 44, no 215–232.

Mostyn, GR & Douglas, KJ 2000, 'Strength of intact rock and rock masses', paper presented at the GeoEng2000 Conference, Melbourne.

Mutaz, E, Serati, M, Bahaaddini, M & Williams, B 2021, 'On the evolution of crack initiation stress threshold', paper presented at The 55th U.S. Rock Mechanics/Geomechanics Symposium, American Rock Mechanics Association, Alexandria.

Nicksiar, M & Martin, CD 2013, 'Crack initiation stress in low porosity crystalline and sedimentary rocks', *Engineering Geology*, vol. 154, pp. 64–76.

Orilogi, E 2019, *Evaluating Volumetric Strain as a Predictor of Yield and Peak Strength for the Multistage Triaxial Test: A Case Study with Utah Coal Specimens*, MSc thesis, Montana Technological University, Butte.

Pagoulatos, A 2004, *Evaluation of Multistage Triaxial Testing on Berea Sandstone*, MSc thesis, The University of Oklahoma, Norman.

Taheri, A, Zhang, Y & Munoz, H 2020, 'Performance of rock crack stress thresholds determination criteria and investigating strength and confining pressure effects', *Construction and Building Materials*, vol. 243.

Tang, C & Hudson, JA 2011, *Rock Failure Mechanisms*, Taylor & Francis, London.

Tapponnier, P & Brace, WF 1976, 'Development of stress-induced microcracks in Westerly granite', *International Journal of Rock Mechanics and Mining Sciences and Geomechanics Abstracts*, vol. 13, pp. 103–112.

Venter, J, Hammah, ECF & Purvis, C 2019, 'New revelations in intact rock strength through automated triaxial testing', paper presented at the 53rd U.S. Rock Mechanics/Geomechanics Symposium, American Rock Mechanics Association, Alexandria.